AD-A130 316 DETERMINATION OF SOIL PROPERTIES THROUGH GROUND MOTION ANALYSIS(U) BALLISTIC MISSILE OFFICE NORTON AFB CA J FRYE ET AL. 29 JUN 83 BMO-82-001 1/1

UNCLASSIFIED F/G 19/4 NL

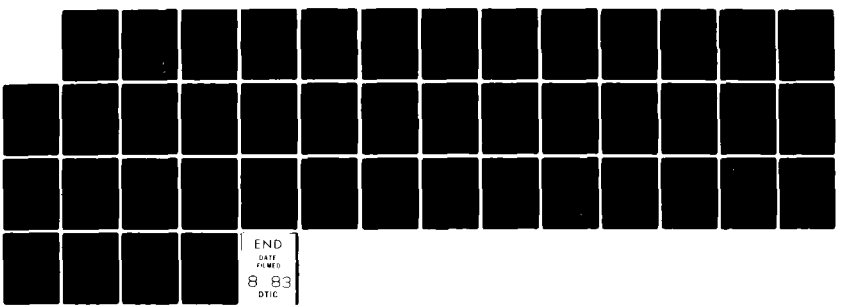

END
DATE FILMED
8 83
DTIC

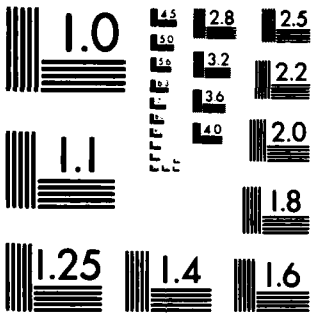

MICROCOPY RESOLUTION TEST CHART
NATIONAL BUREAU OF STANDARDS-1963-A

PHYSICAL MODELING TECHNIQUES FOR MISSILE AND OTHER PROTECTIVE STRUCTURES

AD A130316

Papers Submitted for Presentation During the
American Society of Civil Engineers
National Spring Convention
Las Vegas, April 1982

Sponsored By the ASCE Engineering Mechanics Division
Committee on Experimental Analysis and Instrumentation

Edited By: T. Krauthammer and C. D. Sutton

DTIC FILE COPY

This document has been approved for public release and sale; its distribution is unlimited.

DTIC ELECTE JUL 14 1983 A

83 02 028

DEPARTMENT OF THE AIR FORCE
HEADQUARTERS BALLISTIC MISSILE OFFICE (AFSC)
NORTON AIR FORCE BASE, CALIFORNIA 92409

REPLY TO ATTN OF: PA

29 Jun 83

SUBJECT: Review of Material for Public Release

TO: Mr. James Shafer
Defense Technical Information Center
DDAC
Cameron Station
Alexandria, VA 22314

The following technical papers have been reviewed by our office and are approved for public release. This headquarters has no objection to their public release and authorizes publication.

1. (BMO 81-296) "Protective Vertical Shelters" by Ian Narain, A.M. ASCE, Jerry Stepheno, A.M. ASCE, and Gary Landon, A.M. ASCE.

2. (BMO 82-020) "Dynamic Cylinder Test Program" by Jerry Stephens, A.M. ASCE.

3. (AFCMD/82-018) "Blast and Shock Field Test Management" by Michael Noble.

4. (AFCMD/82-014) "A Comparison of Nuclear Simulation Techniques on Generic MX Structures" by John Betz.

5. (AFCMD/82-013) "Finite Element Dynamic Analysis of the DCT-2 Models" by Barry Bingham.

6. (AFCMD/82-017) "MX Basing Development Derived From H. E. Testing" by Donald Cole.

7. (BMO 82-017) "Testing of Reduced-Scale Concrete MX-Shelters-Experimental Program" by J. I. Daniel and D. M. Schultz.

8. (BMO 82-017) "Testing of Reduced-Scale Concrete MX-Shelters-Specimen Construction" by A. T. Ciolko.

9. (BMO 82-017) "Testing of Reduced-Scale Concrete MX-Shelters-Instrumentation and Load Control" by N. W. Hanson and J. T. Julien.

10. (BMO 82-003) "Laboratory Investigation of Expansion, Venting, and Shock Attenuation in the MX Trench" by J. K. Gran, J. R. Bruce, and J. D. Colton.

11. (BMO 82-003) "Small-Scale Tests of MX Vertical Shelter Structures" by J. K. Gran, J. R. Bruce, and J. D. Colton.

12. (BMO 82-001) "Determination of Soil Properties Through Ground Motion Analysis" by John Frye and Norman Lipner.

13. (BMO 82-062) "Instrumentation for Protective Structures Testing" by Joe Quintana.

14. (BMO 82-105) "1/5 Size VHS Series Blast and Shock Simulations" by Michael Noble.

15. (BMO 82-126) "The Use of Physical Models in Development of the MX Protective Shelter" by Eugene Sevin.

*16. REJECTED: (BMO 82-029) "Survey of Experimental Work on the Dynamic Behavior of Concrete Structures in the USSR" by Leonid Millstein and Gajanen Sabnis.

CAROL A. SCHALKHAM, 1Lt, USAF
Public Affairs Officer

Cy To: Dr. T. Krauthammer
Associate Professor
Department of Civil and
Mineral Engineering
University of Minnesota

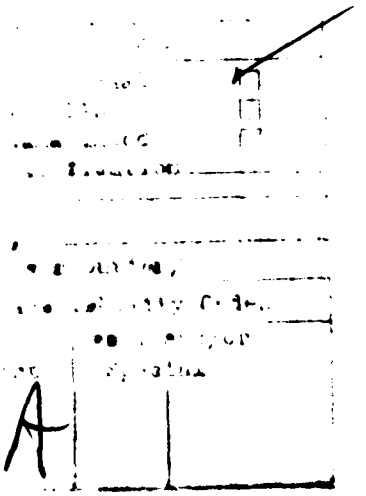

DETERMINATION OF SOIL PROPERTIES THROUGH GROUND MOTION ANALYSIS

John Frye
&
Norman Lipner

5 June, 1981

ABSTRACT

A method of calculating in situ one dimensional stress-strain soil properties from vertical ground motion is presented. The method relies on the fact that superseismic air blast ground surface loadings produce ground motions that are very nearly vertical and one dimensional in character. Therefore the equations of motion that govern the response are simple and may be integrated to obtain one dimensional stress-strain relations. Thus, results from tests that incorporate superseismic air blast surface loading and sensors to measure vertical motion at various depths in the soil can be used to calculate soil stress-strain properties directly. The method accounts for multiple records at a given depth and features techniques for characterizing response histories and interpolating velocities at depths between those where measurements have been made. As an example, for the DISC HEST Test I event, conducted in Ralston Valley, Nevada as part of the MX development program, the site properties are computed based on the free field data.

DETERMINATION OF SOIL PROPERTIES THROUGH GROUND MOTION ANALYSIS

J. W. Frye[1] and N. Lipner[2], M. ASCE

INTRODUCTION

The ground response to overhead highly superseismic airblast loading (airblast shock speed faster than ground shock speeds) is nearly one-dimensional uniaxial strain and the motions are nearly vertical. Soil properties for prediction of these motions have typically been determined from dynamic uniaxial strain laboratory tests. However, the process of extracting soil samples from the field can disturb the material and, as a result, the laboratory properties could be different from the in situ material behavior.

An approach to determine the in situ properties is to perform a field test where the ground surface is loaded by superseismic airblast. Data from sensors that measure vertical motion at various depths in the ground could then be used to calculate the uniaxial strain properties of the soil by use of the one-dimensional equation of motion.

One type of surface loading that has been used to obtain a one-dimensional response is the DISC (Dynamic In Situ Compressibility) HEST (High Explosive Simulation Technique) test shown in Figure 1. This test employs a circular region of explosives that is center detonated. The detonation propagates outward fast enough that the early-time response to peak velocity is essentially one-dimensional within some region under the loaded area that is governed by the disc radius and the soil properties. Because of the finite propagation velocity, time at any range from the centerline is measured with respect to the arrival of the overhead airblast at that range.

---

1. Member of the Technical Staff, Hardness and Survivability Laboratory, TRW, Redondo Beach, CA 90278

2. Department Head, Hardness and Survivability Laboratory, TRW, Redondo Beach, CA 90278

ANALYSIS FORMULATION

The one-dimensional equation of motion relates the vertical normal stress gradient to the acceleration of the soil.

$$\frac{\partial \sigma_z}{\partial z} = \rho \ddot{u}_z \tag{1}$$

Here z is the vertical coordinate (Fig. 1), σ_z is the normal stress in the z direction (tensile stress is positive), and ρ is the soil density. Equation (1) can be integrated with respect to depth from the ground surface to a depth z to obtain the following equation for stress:

$$\dot{\sigma}_z = -p(t) + \int_0^z \rho \dot{v}_z dz \tag{2}$$

where the constant of integration, $p(t)$, is the surface pressure-time history, a boundary condition of the problem, and the first time derivative of velocity, $\dot{v}_z$, replaces the second time derivative of displacement.

The one-dimensional strain, ϵ_z, is the derivative of the vertical displacement with respect to depth.

$$\epsilon_z = \frac{\partial u_z}{\partial z} \tag{3}$$

Taking the time derivative of Equation (3) provides the following relation for the strain rate $\dot{\epsilon}_z$:

$$\dot{\epsilon}_z = \frac{\partial \dot{u}_z}{\partial z} = \frac{\partial v_z}{\partial z} \tag{4}$$

and integrating Equation (4) gives the following relation for strain in terms of velocity:

$$\epsilon_z = \int_0^t \frac{\partial v_z}{\partial z} dt \tag{5}$$

The constant of integration is zero because the strain in the soil is

measured with respect to the geostatic strain and, therefore, is zero at time zero.

From Equations (2) and (5) it is seen that if the vertical component of velocity is defined with respect to time and depth, then stress and strain may be directly calculated from derivatives of the velocity by performing integrations with respect to depth and time. The pressure time history at the surface and estimates of the soil density are also required by Equation (2).

Evaluation of the integrals of Equations (2) and (5) requires knowledge of the velocity field for the complete space-time region of interest. In a test, motion sensors at only a limited number of depths can be implanted because of cost, as well as physical constraints. Therefore, a method must be developed to interpolate from the data available for a limited number of depths to the velocity history at any depth.

In many test events, more than one record is available at some depths, so that if one sensor is faulty, all of the velocity-time information concerning that particular depth is not lost. Data records available for a particular depth will vary from one another due to a number of reasons, such as variation from one location to another of soil properties and surface pressure-time histories. In examining the velocity-time records taken at a particular depth, it is not always obvious that one particular record is the most accurate and representative of all. Thus, some method of including all acceptable records taken at a particular depth must be employed in defining the velocity-time history to be used in the interpolation process. Clearly some records that show anomalous results, not representative of motions that are physically plausable, should be excluded from consideration Such records might be taken from sensors that either were poorly installed,

were destroyed by the shock loading, or produced records that were extremely noisy.

The method chosen for interpolating the measured velocity records uses a transformed coordinate system with a time-like coordinate s that remains constant with depth along specific characteristics of the velocity time history. At the beginning of motion, s is always taken as zero; at peak velocity, s equals 1.0; and at the end of the velocity record, s assumes some large value such as 10. Other values of s are chosen to follow percentages of the peak velocity, as shown in Figure 2. Mathematically, the transformation is as follows:

$$z' = z$$
$$s = f(z,t) \qquad (6)$$

where z' is the depth coordinate of the new coordinate system.

This transformation is piecewise linear between depths where velocity records are available. Averaged characteristic information available from the records at each depth is used. At constant depth, the time-like coordinate s is related to t through a series of straight line segments between s and t values established for particular velocity record characteristics. Details of the formulation of the transformation and other matters concerning the interpolation between records at different depths are given in the appendix.

The interpolation of the velocity between depths where data are available is done in the z', s coordinate system along lines of constant s values; i.e., the interpolation is performed with respect to specific velocity record characteristics. Peak velocities at adjacent depths where data are available are used to interpolate the peak velocity at in-between depths. Thus, half-peak velocity data are used to interpolate half-peak velocities,

and so on.

In order to establish a unique definition of the velocity history at a given depth, the velocity record is broken up into a series of segments that begin and end at specific s coordinates. The segments are taken to be the same at all depths forming a grid work in the z', s space as shown in Figure 3. The velocity history at each depth and over each segment is represented as a cubic function with the beginning and end of each segment having the same velocity value as adjacent segments so that step changes in velocity (infinite acceleration) are ruled out. The parameters of the cubic interpolation functions are evaluated based on a least square fit to the velocity records at the depth in question.

Interpolation between depths is done using an exponential function that begins at the adjacent upper depth and ends on the adjacent lower depth. Extrapolation of velocities to depths above the shallowest depth for which data are available is performed by extrapolating the exponential interpolation function derived for the region between the two shallowest depths. Velocity at depths below the deepest depth for which data are available is obtained, in a similar manner, from the interpolation function of the two deepest depths.

Having established a method of deriving unique velocity records for all depths and times from the measured data, stresses and strains are calculated from Equations (2) and (5) using central differencing and standard numerical integration techniques. The results of the analysis have been found to be rather insensitive to the discretization used in the numerical analysis. The major factors in the analysis appear to be the choice of velocity histories and of interpolation segments.

ANALYSIS RESULTS

Soil stress strain relations have been calculated from one-dimensional finite difference calculation results, as a check on the analysis, and from DISC HEST test data. The finite difference calculation considered two dry soil layers over a wet soil half-space (Reference 1). The dry soil layers had linear loading and linear unloading moduli. The loading modulus for the lower dry soil material was 1.5 times as stiff as for the surface layer; the unloading moduli in both layers were about an order of magnitude stiffer than the loading (Fig. 4). The velocity histories from the calculation were input into the analysis developed herein, with the stress-strain curve results shown in Figure 4. For this analysis, velocity histories were used at every 1.83 m (6 ft) of depth from the surface down to 18.29 m (60 ft) and every 3.05 m (10 ft) of depth from 18.29 m (60 ft) down to 45.72 m (150 ft).

The technique is able to track properties that change with depth and is able to follow unloading along entirely different slopes than the loading curve. The unloading results are less satisfactory than those for the loading portion of the response. However, because the unloading is so steep, a small change in strain can make a large difference in the slope of the curve. The results also show that the method predicts a gradual, rather than a sharp, change in properties with depth. This is attributed to smoothing and other approximations inherent in the use of exponential and cubic functions to perform the required interpolations.

When using theoretical results, velocity records are available at the surface as well as at large depths. With experimental data, surface velocity histories are not known and histories at deep depths are likely to be influenced by free surface reflections from outside the loaded area that produce multi-dimensional response characteristics.

After gaining experience with the technique using analytical results, it was then applied to data from the DISC HEST Test I event (Reference 2) conducted in Ralston Valley, Nevada. The HEST cavity radius on this test was 13.7 m (45 ft), and data was obtained at eight depths down to 15.2 m (50 ft) (Fig. 5). The data appeared to be relatively free of noise, allowing most of the records to be incorporated in the evaluation of the velocity field history. A total of fourteen records over the eight depths (Fig. 6) were included in the analysis. Figure 7 shows a family of interpolated velocity histories obtained from the analysis.

The airblast pressure history was measured at several points on the ground surface within the HEST cavity. A best fit through the pressure records (Reference 2) is shown in Figure 8. This pressure history was initially used in Equation (2) to calculate stress histories at depths of interest, but unsatisfactory results were obtained. The main problem was that, at the onset of incipient motion ($s = 0$) at some depths, the stress was nonzero because the two terms on the right hand side of Equation (2) did not exactly cancel. This occurred because the averaged surface overpressure and the velocity field interpolated from the data were not completely consistent.

An alternate approach is to compute a surface pressure loading from the velocity field. Setting the stress equal to zero in Equation (2)

at the arrival of motion at any depth, d_0 yields

$$0 = -p(t) + \int_0^{d_0(t)} \rho \dot{v}_z \, dz$$

$$p(t) = \int_0^{d_0(t)} \rho \dot{v}_z \, dz \tag{7}$$

A pressure history derived from the ground motion response is shown in Figure 8 compared with the best fit pressure history. The pressure histories agree reasonably well in the early time of the motion. The initial slope of the calculated pressure loading is not as steep as that obtained from measurements. This is probably due to smoothing of the velocity histories by the interpolation process and the difficulty of exactly predicting ground motion at and near the surface from measurements made below the surface. The impulse histories of the measured and calculated surface loadings are also shown in Figure 8. They compare very well in the early time of the motion indicating that the interpolation process averages out variations in the velocity histories in a manner that preserves the overall character and energy content of the response. After about 25 ms of response, the calculated and measured pressure and impulse histories begin a significant divergence. This can be attributed to the reduction of the vertical ground accelerations by edge effects. The divergence of the pressure histories may serve as a time marker for the demarcation of when two-dimensional response becomes important.

Examination of the data in Figure 7 shows that peak velocity is achieved within 25 ms down to a depth of about 8 m. For larger depths, the time to peak velocity increases with depth at a faster rate than might be expected for one-dimensional response. Information on properties at deeper depths can be obtained from two-dimensional finite difference calculations, however, assumptions are required to obtain the uniaxial strain properties at the depths because the response is two-dimensional and essentially only vertical motion records are available.

Figure 9 shows the interpolated uniaxial strain stress-strain plots obtained from the velocity field and the derived surface overpressure. The initial slope of the stress-strain curves and the 4 MPa secant modulus are plotted as a function of depth in Figure 10 and compared with the seismic velocity profile of the site. The loading properties show relatively small variation with depth down to 9 m. The unloading properties are not well behaved, but most of the unloading occurs after the 25 ms of one-dimensional simulation time.

The initial slope of the interpolated stress-strain curves produces a modulus that compares better with the seismic results (except very near the surface) than does the 4 MPa modulus. This is to be expected since the moduli obtained from seismic measurements are representative of the soil response at very low stress values. The 4 MPa modulus is consistently lower than the seismic or initial slope values. This reflects the softening of the soil with increasing stress, characteristic of cemented granular soil.

The seismic profile shows a soft soil layer in the top 1.5 m (5 ft) that is not present in the results of the interpolated stress-strain curves. It is possible that the material is behaving stiffer than would be expected from the seismic profile, because of strain rate effects. However, the

fact that the interpolated peak surface pressure is lower than (about 15 percent) the averaged pressure gage data indicates that the near surface motions were actually larger than those used in the analysis, which would result in softer near surface properties.

Better results might be obtained by making use of seismic velocity information in extrapolating velocity field data to obtain surface values. The second depth that velocity data was recorded in DISC HEST Test I was at 1.5 m, the same depth that a sudden hardening of soil modulus was indicated by seismic data. Thus the second velocity history occured at a transition region in soil properties. The velocity response at this depth then contained information that was more characteristic of the soil below the transition boundary. Therefore, the extrapolation of motion field to the surface was influenced by the second seismic layer. An alternate approach to performing the extrapolation would be to increase the peak surface velocity until the interpolated peak surface pressure was in agreement with the data. In cases where it is important to more accurately define the material properties in this very near surface layer, then gages at two depths within the layer (such as 0.5 and 1.0 m) should be used in the experiment.

CLOSURE

The purpose of this paper is to demonstrate a methodology for determining uniaxial strain mechanical properties of soil solely from velocity time histories obtained from a high explosive field test event. It is similar to the LASS (Lagrangian Analysis of Stress and Strain) methodology developed by SRII (Reference 3) for analysis of spherical motions. However, for the spherical case both stress and velocity data are needed.

Analysis of in situ field test data is generally the most accurate technique for determining in situ mechanical properties. The material property inversion technique described herein represents a first step in the analysis of the data; the complete development of properties at a site would consider all available relevant information, such as seismic and laboratory test results. The properties derived from in situ data might then be smoothed or adjusted based on auxiliary data, as long as these changes were within the uncertainties of the in situ analysis. These revised properties would then be used in one- and two-dimensional finite difference calculations to verify their adequacy.

CONCLUSIONS

(1) Dynamic stress-strain properties of in situ soil may be derived directly from velocity histories taken from surface pressure loading tests, using the method described herein, down to depths where the ground motion is sufficiently one-dimensional. Results have been obtained from experimental data for the DISC HEST Test I event.

(2) Surface pressure histories may be derived from the velocity data for the duration of one-dimensional response. This can provide a check on the consistency between pressure and velocity data. The time when the measured and derived surface pressure loading diverges is an indication of the duration of one-dimensional response. In the DISC HEST Test I event, the measured and derived impulse histories were in reasonable agreement out to about 25 ms.

(3) The interpolation functions used in the technique are effective in deriving soil velocity as a continuous function of depth and time. Since the functions are based on measured rather than hypothesized soil response characteristics they should be able to be applied to tests with different soil types with equal success. This approach can also be generalized to apply to motion fields that are dependent on two spacial coordinates.

ACKNOWLEDGEMENT

This work was performed for the USAF Ballistic Missile Office under the direction of Lt. Col. Donald H. Gage. We acknowledge the support of Dr. J. S. Zelasko of the US Army Engineer Waterways Experiment Station who provided us the DISC HEST Test I field test data and the finite difference calculational results.

Appendix I - Derivation of Coordinate Transformation and Interpolation Functions

There are a number of characteristic times that are clearly important in describing a velocity record (Fig. 2). The two times of dominant importance are the time when the motion begins and the time when the velocity reaches its greatest absolute amplitude. Other points such as the end of the record and time where the velocity attains given fractions of the peak velocity serve to complete a listing of the important characteristic time points of the record. The points that serve to best describe the records may be assigned labels that we will denote by the symbol s. For convenience, the labels can be made numeric and assigned values that increase with time for a given record. By convention the start of motion is at s=0; the peak velocity is at s=1.0; and the end of the record is assigned a large number such as s=10. Points between the peak velocity and the end of the record have s values between 1 and 10 and points between the start of motion and the peak velocity have s values between 0 and 1.

Once a set of s labels have been chosen they can be applied to all of the records at all of the depths. The value of s remains constant with depth along a characteristic line connecting similar time points of different records. At a given depth, points with particular values of s form clusters. The best estimate of where particular s points ought to fall can be obtained by calculating mean values.

$$\bar{t}(z_i, s) = \frac{1}{n_i} \sum_{j=i}^{n_i} t_j(z_i, s) \qquad \text{(A-1)}$$

where $t(z_i, s)$ is the time of characteristic point s at depth z_i and record j; $\bar{t}(z_i, s)$ is the average time of characteristic point s for depth z_i; and n_i is the number of records at depth z_i.

To estimate values of s between depths where records exist, a straight line can be drawn between the average time of the various s labels for existing records. In this way, a family of segmented constant s curves may be obtained, which can be considered as a new time-depth coordinate system. Specific features of the velocity response history, for each depth, occur at constant values of the time like s coordinate. The symbols of the new coordinates z', s are related to the z, t coordinates by the following transformation relations.

$$z' = z \qquad \text{(A-2)}$$
$$s = f(z, t)$$

In order to further define the function $f(z,t)$ the variation of s as a function of t at a given depth must be specified. The simplest choice, and the one that will be shown here, is to let s vary as a linear function of t between each of the labeled values of s. The linear function has the advantage that it guarantees that a unique mapping of s onto t coordinates exists and vice versa. This linear relation between s and t is illustrated

in Figure A-1 and shown in equation form below

$$s = s^{(i)} + (s^{(i+1)} - s^{(i)}) \frac{[t-\bar{t}(z,s^{(i)})]}{[\bar{t}(z,s^{(i+1)}) - \bar{t}(z,s^{(i)})]} \qquad \text{(A-3)}$$

$$\text{for } \bar{t}(z,s^{(i)}) \le t \le \bar{t}(z,s^{(i+1)})$$

where $s^{(i)}$ is the value of s at the i'th characteristic point on the velocity history. Equation (A-3) can be rearranged to give the solution of t as a function of s.

$$t = \bar{t}(z,s^{(i)}) + \frac{[\bar{t}(z,s^{(i+1)})-\bar{t}(z,s^{(i)})](s-s^{(i)})}{(s^{(i+1)}-s^{(i)})} \qquad \text{(A-4)}$$

$$\text{for } s^{(i)} \le s \le s^{(i+1)}$$

The terms $\bar{t}(z^{(i)},s)$ are linear functions of depth. In equation form the relation for $\bar{t}(z,s^{(i)})$ is

$$\bar{t}(z,s^{(i)}) = \bar{t}(z_j,s^{(i)}) + \frac{[\bar{t}(z_{j+1},s^{(i)})-\bar{t}(z_j,s^{(i)})](z-z_j)}{(z_{j+1}-z_j)} \qquad \text{(A-5)}$$

$$\text{for } z_j \le z \le z_{j+1}$$

Equations (A-3) and (A-5) define the function $f(z,t)$ of equation (A-2). The inverse transformation equation is

$$z = z' \qquad \text{(A-6)}$$
$$t = g(z',s)$$

The advantage of the coordinate system is that it provides a convenient framework for interpolating velocities between depths. Points at s=1 will be related to peak velocity values only; points with s=1/2 will be related to velocity values that are at 1/2 of the peak value, and so forth.

At each depth a variety of records are typically available. For those records at a given depth that are valid, we have the problem of forming a function that is representative of the velocity response history. Since the records are complex it is impractical to consider

using one equation to represent the entire time history at a given depth. An equation of this kind would likely be complicated and might vary in form depending on the depth. A more realistic approach is to segment the velocity record and treat each segment independently of the other but at the end points of a segment have velocity values that match up with those of adjacent segments. For convenience we will require that common s values be used to define segment boundaries. It is usually better to have a larger number of segments to define the history at the beginning of the motion than at the end of the velocity record. The time history at the beginning of the motion changes more rapidly than at the end and thus should be more carefully described.

Lagrangian interpolation functions are particularly well suited for establishing the velocity histories for the various segments of the response at a particular depth. These kinds of functions can be readily defined to any desired order, but the higher order functions have unfavorable properties. Since the function must describe the velocity history over only a segment of the total time of the record, a cubic function should be adequate to give a good description of the required motion. The general form of a cubic Lagrangian interpolation function is as follows:

$$w_{ij}(s) = \frac{(a_{i2}-s)(a_{i3}-s)(a_{i4}-s)\,v_{ij1}}{(a_{i2}-a_{i1})(a_{i3}-a_{i1})(a_{i4}-a_{i1})} + \frac{(a_{i1}-s)(a_{i3}-s)(a_{i4}-s)\,v_{ij2}}{(a_{i1}-a_{i2})(a_{i3}-a_{i2})(a_{i4}-a_{i2})} + \frac{(a_{i1}-s)(a_{i2}-s)(a_{i4}-s)\,v_{ij3}}{(a_{i1}-a_{i3})(a_{i2}-a_{i3})(a_{i4}-a_{i3})} + \frac{(a_{i1}-s)(a_{i2}-s)(a_{i3}-s)\,v_{ij4}}{(a_{i1}-a_{i4})(a_{i2}-a_{i4})(a_{i3}-a_{i4})} \tag{A-7}$$

Here v_{ij1}, v_{ij2}, v_{ij3} and v_{ij4} are the velocities at each of four s coordinate locations a_{i1}, a_{i2}, a_{i3} and a_{i4} within segment i and at depth j, and w_{ij} is the function defining the velocity history for the i'th segment and j'th depth. The locations a_{i1} and a_{i4} will be considered to occur at the

beginning and end of segment i.

At the point where s is zero, the value of velocity is zero also. This is always true by definition since the s=0 point is taken to be the point in time where the motion response begins. Thus, for the first interpolation segment between s=0 and s=s_1, where s_1 is the value at the end of the first segment, the value v_{ij1} is zero. The values v_{ij2}, v_{ij3} and v_{ij4} are still unknown.

For any given time history at a particular depth, errors will occur between the velocity given by Equation (A-7) and the time history value. For a given value s the error can be written as

$$E_{jk}(s) = V_{jk}(s) - w_{ij}(s) \qquad \text{(A-8)}$$

or

$$E_{jk}(s) = V_{jk}(s) - h_{i1}v_{ij1} - h_{i2}v_{ij2} - h_{i3}v_{ij3} - h_{i4}v_{ij4} \qquad \text{(A-9)}$$

where $V_{jk}(s)$ and $E_{jk}(s)$ are the velocity and velocity error, respectively, for time history k at coordinate s and depth j and

$$h_{i1} = \frac{(a_{i2}-s)(a_{i3}-s)(a_{i4}-s)}{(a_{i2}-a_{i1})(a_{i3}-a_{i1})(a_{i4}-a_{i1})}$$

$$h_{i2} = \frac{(a_{i1}-s)(a_{i3}-s)(a_{i4}-s)}{(a_{i1}-a_{i2})(a_{i3}-a_{i2})(a_{i4}-a_{i2})}$$

$$h_{i3} = \frac{(a_{i1}-s)(a_{i2}-s)(a_{i4}-s)}{(a_{i1}-a_{i3})(a_{i2}-a_{i3})(a_{i4}-a_{i3})} \qquad \text{(A-10)}$$

$$h_{i4} = \frac{(a_{i1}-s)(a_{i2}-s)(a_{i3}-s)}{(a_{i1}-a_{i4})(a_{i2}-a_{i4})(a_{i3}-a_{i4})}$$

The error value $E_{jk}(s)$ may be either positive or negative; however, only the absolute amplitude of the error value is of importance. The square of the error value $E_{jk}(s)$ is always positive and is then a better

error measure for the purposes of judging the ability of the function $w_{jk}(s)$ to fit the velocity-time response $V_{jk}(s)$.

The total error is not just that measured at one coordinate value for one record but is the integral for all points s over the segment summed for all of the records available at a given depth.

$$E_{Tji} = \sum_{k=1}^{n_j} \int_{s_{i-1}}^{s_i} E_{jk}(s)ds \tag{A-11}$$

$$E_{Tji} = \sum_{k=1}^{n_j} \int_{s_{i-1}}^{s_i} [V_{jk}(s) - h_{i1}v_{ij1} - h_{i2}v_{ij2} - h_{i3}v_{ij3} - h_{i4}v_{ij4}]^2 ds \tag{A-12}$$

We must select velocities v_{ij2}, v_{ij3}, and v_{ij4} that minimize the total error E_{Tji}. We will assume that the value v_{ij1} is always constrained by continuity requirements with segment $i-1$. If we evaluate the segments in order starting with $i=1$, we need only match the constant v_{1j4} for segment 1 with the constant v_{2j1} for segment 2 to preserve continuity of velocity between segment 1 and 2. The constant v_{1j1} is always zero since it corresponds to the beginning of motion. In evaluating the constants for segment 1, we need only find values for v_{1j2}, v_{1j3} and v_{1j4}. If v_{1j4} is set equal to v_{2j1} then for the second segment only the values v_{2j2}, v_{2j3} and v_{2j4} need be evaluated. The process can be continued for all of the segments.

The positions a_{i1} and a_{i4} then must fall at the beginning and end of the segment. Thus $a_{i1} = s_{i-1}$ and $a_{i4} = s_i$. The points a_{i2} and a_{i3} can be chosen as equally spaced along the segment. Thus

$$\begin{aligned} a_{i1} &= s_{i-1} \\ a_{i2} &= s_{i-1} + \tfrac{1}{3}(s_i - s_{i-1}) \\ a_{i3} &= s_{i-1} + \tfrac{2}{3}(s_i - s_{i-1}) \\ a_{i4} &= s_i \end{aligned} \tag{A-13}$$

The error function E_{Tji} is always positive and is a quadratic function of the terms v_{ij2}, v_{ij3} and v_{ij4}. It follows that its minimum occurs where the derivatives of E_{Tji} with respect to v_{ij2}, v_{ij3} and v_{ij4} are all zero. These conditions produce the equations for the determination of the unknown velocity constants.

$$\frac{\partial E_{Tji}}{\partial v_{ij2}} = 0 = \sum_{k=1}^{n_j} \int_{s_{i-1}}^{s_i} [-V_{jk}h_{i2} + h_{i1}h_{i2}v_{ij1} + h_{i2}^2 v_{ij2} + h_{i2}h_{i3}v_{ij3} + h_{i2}h_{i4}v_{ij4}]ds \tag{A-14}$$

$$\frac{\partial E_{Tji}}{\partial v_{ij3}} = 0 = \sum_{k=1}^{n_j} \int_{s_{i-1}}^{s_i} [-V_{jk}h_{i3} + h_{i1}h_{i3}v_{ij1} + h_{i2}h_{i3}v_{ij2} + h_{i3}^2 v_{ij3} + h_{i3}h_{i4}v_{ij4}]ds \tag{A-15}$$

$$\frac{\partial E_{Tji}}{\partial v_{ij4}} = 0 = \sum_{k=1}^{n_j} \int_{s_{i-1}}^{s_i} [-V_{jk}h_{i4} + h_{i1}h_{i4}v_{ij1} + h_{i2}h_{i4}v_{ij2} + h_{i3}h_{i4}v_{ij3} + h_{i4}^2 v_{ij4}]ds \tag{A-16}$$

Evaluating each term of the summation and integration processes of Equations (A-14), (A-15) and (A-16) separately and placing terms of known value on the right hand side of the equation with terms of unknown value on the left hand side of the equation produces the following results:

$$\begin{aligned} c_{22}v_{ij2} + c_{23}v_{ij3} + c_{24}v_{ij4} &= F_2 \\ c_{23}v_{ij2} + c_{33}v_{ij3} + c_{34}v_{ij4} &= F_3 \\ c_{24}v_{ij2} + c_{34}v_{ij3} + c_{44}v_{ij4} &= F_4 \end{aligned} \tag{A-17}$$

where

$$c_{22} = \sum_{k=1}^{n_j} \int_{s_{i-1}}^{s_i} h_{i2}^2 ds \qquad \text{(A-18)}$$

$$c_{23} = \sum_{k=1}^{n_j} \int_{s_{i-1}}^{s_i} h_{i2} h_{i3} ds \qquad \text{(A-19)}$$

$$c_{24} = \sum_{k=1}^{n_j} \int_{s_{i-1}}^{s_i} h_{i2} h_{i4} ds \qquad \text{(A-20)}$$

$$c_{33} = \sum_{k=1}^{n_j} \int_{s_{i-1}}^{s_i} h_{i3}^2 ds \qquad \text{(A-21)}$$

$$c_{34} = \sum_{k=1}^{n_j} \int_{s_{i-1}}^{s_i} h_{i3} h_{i4} ds \qquad \text{(A-22)}$$

$$c_{44} = \sum_{k=1}^{n_j} \int_{s_{i-1}}^{s_i} h_{i4}^2 ds \qquad \text{(A-23)}$$

$$F_2 = \sum_{k=1}^{n_j} \int_{s_{i-1}}^{s_i} (V_{jk} h_{i2} - h_{i1} h_{i2} v_{ij1}) ds \qquad \text{(A-24)}$$

$$F_3 = \sum_{k=1}^{n_j} \int_{s_{i-1}}^{s_i} (V_{jk} h_{i3} - h_{i1} h_{i3} v_{ij1}) ds \qquad \text{(A-25)}$$

$$F_4 = \sum_{k=1}^{n_j} \int_{s_{i-1}}^{s_i} (V_{jk} h_{i4} - h_{i1} h_{i4} v_{ij1}) ds \qquad \text{(A-26)}$$

Equations (A-17) are a set of three linear relations with constant coefficients and three unknowns that can be readily solved. The solution is not a major problem once the constant coefficients c_{22}, c_{23}, etc., and the right hand side constants F_2, F_3 and F_4 are known. However, these constants require an integration that is not trivial. The functions h_{i1}, h_{i2}, h_{i3} and h_{i4} are not simple, and the velocity functions V_{jk} are typically defined at a finite number of points rather than in a continuous manner due to the digital definition of the record. The integrations for the coefficients of the equation can be carried out numerically with no difficulty since the functions are defined for all values s within the segment. A standard procedure for performing the numerical integration is to divide up the segment into a large number of intervals, and then evaluate the integral based on the function values at the beginning and end of each of the intervals.

For the integration of the constants F_2, F_3 and F_4, it will be necessary to define values of V_{jk} at points s where digitized velocity data are undefined. This problem is resolved by assuming that the velocity in each record varies linearly between the defined values. Figure A-1 illustrates the assumed

variation of the velocity record with respect to s and time. By making the assumption of linearity between the defined velocity record points, the velocity record becomes in effect defined at all points and the integrations of Equations (A-24), (A-25) and (A-26) can be carried out to obtain the constants F_2, F_3 and F_4.

With the determination of the constants v_{ijk} for all segments at all depths, a set of velocity records are available at each depth that are representative of an optimal average of all valid velocity records. The problems now remaining are how to interpolate between depths where velocity records are recorded and also how to interpolate from the velocity record at the shallowest depth up to the surface and to depths below the deepest where data is available.

There are any number of schemes that could be applied to the interpolation of the velocity records between depths. One could use linear, quadratic, cubic or higher order polynomials, or one could use functions that are appealing on a physical basis. Since some characteristics of velocity histories are known to decay in an approximately exponential manner with depth within a given material, exponential functions should provide useful vehicles for interpolating the velocity records. After some experimentation, it was found that the exponential functions in fact produced more favorable results than the polynomial functions. The major drawback to the polynomial functions is their tendency to oscillate. This oscillation produces velocity responses that can increase with respect to depth instead of decrease even though all of the points used in the interpolation show a decrease in velocity with respect to depth.

The simplest type of exponential fit involves placing an exponential function between two points. Suppose it is required to determine the

variation of velocity between depths j and $j+1$ along a time-like coordinate line s. Using Equation (A-7), the velocities $w_{i(j+1)}$ and w_{ij} are obtained. The equation must then satisfy the following constraints.

$$\begin{aligned} w_{ij} &= e^{(a+bz'_j)} \\ w_{i(j+1)} &= e^{(a+bz'_{j+1})} \end{aligned} \tag{A-27}$$

The constants a and b are unknown and z'_j and z'_{j+1} are the depth values at depths j and $j+1$. The equation can be solved for a and b by taking the log of both sides of the equation.

$$\begin{aligned} \log w_{ij} &= a + bz'_j \\ \log w_{i(j+1)} &= a + bz'_{j+1} \end{aligned} \tag{A-28}$$

Solving for a and b produces the following

$$a = \frac{z'_{j+1} \log (w_{ij}) - z'_j \log (w_{i(j+1)})}{(z'_{i+1} - z'_i)} \tag{A-29}$$

$$b = \frac{\log (w_{i(j+1)}) - \log (w_{ij})}{(z'_{i+1} - z'_i)} \tag{A-30}$$

Knowing the constants a and b, the velocity $w(z')$ is solved from the relation

$$w(z') = e^{(a+bz')} \qquad (z'_{j+1} \leq z' \leq z'_j) \tag{A-31}$$

A special problem arises when the velocities are negative or change sign between depths. In the case of negative velocities w_{ij} and $w_{i(j+1)}$ in Equation (A-29) and (A-30) are replaced by absolute values and the sign of the right hand side of Equation (A-31) is made negative instead of positive. In the case where the velocity changes sign a new velocity term $w'(z')$ is defined by adding or subtracting from $w(z')$ a constant equal to twice the absolute value of the velocity at the lower depth point.

$$w'(z') = w(z') \pm 2|w_{i(j+1)}| \qquad \text{(A-32)}$$

For instance if $w(z'_j)$ is negative and $w(z'_{j+1})$ is positive then $2|w_{i(j+1)}|$ is subtracted from $w(z')$ to compute $w'(z')$. $w(z'_{j+1})$ would then be equal to $-w_{i(j+1)}$. The experimental interpolation is computed in terms of $w'(t')$ which always has the same sign. $w(z')$ is calculated from $w'(t')$ by appropriately adding or subtracting the constant $2|w_{i(j+1)}|$ from $w'(z')$.

$$w(z') = w'(z') \mp 2\, w_{i(j+1)} \qquad \text{(A-33)}$$

The selection of the constant $2|w_{i(j+1)}|$ is arbitrary but is not a critical one since sign changes in velocity occur at late times in the velocity histories where soil motions are not critical in determining loading slopes of the soil stress-strain behavior.

To extrapolate velocities to the surface, the velocity records of the two shallowest depths must be used. The only piece of information available at the surface is the time of the start of the pressure loading. The first s label line at s=0 can then be drawn from the first depth to this point at the surface. The s label at s=1 should fall no more than a millisecond behind the label for s=0 since the rise time of the blast loading is very short. The s labels falling after s=1 can be extended up to the surface based on their slope between the two shallowest depths. These considerations are illustrated in Figure (A-2).

Having established the s coordinates for extrapolating the velocity, it remains to establish how the velocity varies in the upper layer of soil. The recommended approach is to simply extend the exponential velocity fit between the two shallowest depths. If the exponential form of the function has a physical basis then this form ought to be the best possible to use given no other information about the velocity in this

region. In a similar manner the two lowest depths with data are used to extrapolate down below the region where information is available.

The velocity time history for all times and depths is thus obtained by three fundamental steps. First, a coordinate transformation between z,t and z',s coordinates is established where certain s values relate to particular features of the velocity-time record. Second, a set of cubic Lagrangian velocity functions are established at each depth to fit a set of velocity records using a least square error criteria. Third, an exponential function is used to extrapolate velocity values from the Lagrangian function along lines of constant s between depths where the velocity functions are defined.

Appendix II - Notation

The following symbols are used in this paper:

$a_{i1}, a_{i2}, a_{i3}, a_{i4}$ = time-like s coordinate locations within interpolation segment i.

a, b = Unknown constants in the evaluation of the exponential function used to interpolate between depths.

c_{ij} = coefficients of set of linear equations used in least square solution for v_{ijk}.

$d_o(t)$ = shallowest depth at time t where soil motion and stress due to soil motion are zero.

$E_{jk}(s)$ = error between velocity record j at depth k and Lagrangian interpolation function for time-like coordinate s.

$f(z,t)$ = function defining time like coordinate s in terms of z and t.

$g(z',s)$ = function defining time t in terms of z' and s.

$h_{i1}, h_{i2}, h_{i3}, h_{i4}$ = components of Lagrangian interpolation functions $w_{ij}(s)$.

n_i = the number of records at depth i.

p = pressure at surface

s = time-like coordirate that remains constant with depth for particular features of the velocity response history.

s_i, s_{i-1} = time-like coordinates at the beginning and end of interpolation segment i.

t = time

$\bar{t}(z_i, s)$ = the average time of characteristic point s for depth z_i.

$t_j(z_i, s)$ = the time of characteristic point s for depth z_i and record j.

u_z = displacement in vertical direction (positive direction is up).

$V_{jk}(s)$ = velocity of record j and depth k for time-like coordinate s.

Appendix II - Notation (continued)

v_t = velocity in vertical direction (positive direction is down).

$v_{ij1}, v_{ij2}, v_{ij3}, v_{ij4}$ = velocity values used with Lagrangian interpolation function for interpolation segment i at depth j.

$w_{ij}(s)$ = Langrangian interpolation function written in terms of time-like coordinate s for interpolation segment i at depth j.

z = vertical coordinate (positive direction is down) [(z,t) coordinate system].

z' = vertical coordinate (z',s) coordinate system

ρ = soil density

σ_z = normal stress in z direction (tensile stress is positive).

Appendix III - References

1. Zelasko, J. S., "Sensitivity of MX-Relevant Vertical Ground Shock Environments to Depth to Groundwater and Soil Compressibility Variations", U.S. Army Engineer Waterways Experiment Station, April, 1980.

2. Jackson, A. E., et al, "Ralston Valley Soil Compressibility Study: Quick-Look Report for DISC Test I", U.S. Army Engineer Waterways Experiment Station Structures Laboratory, Vicksburg, Mississippi, May, 1981.

3. Gradv, D. E., et al, "In Situ Constitutive Relations of Soils and Rocks", DNA 3671Z, SRI International, Menlo Park, California, March, 1974.

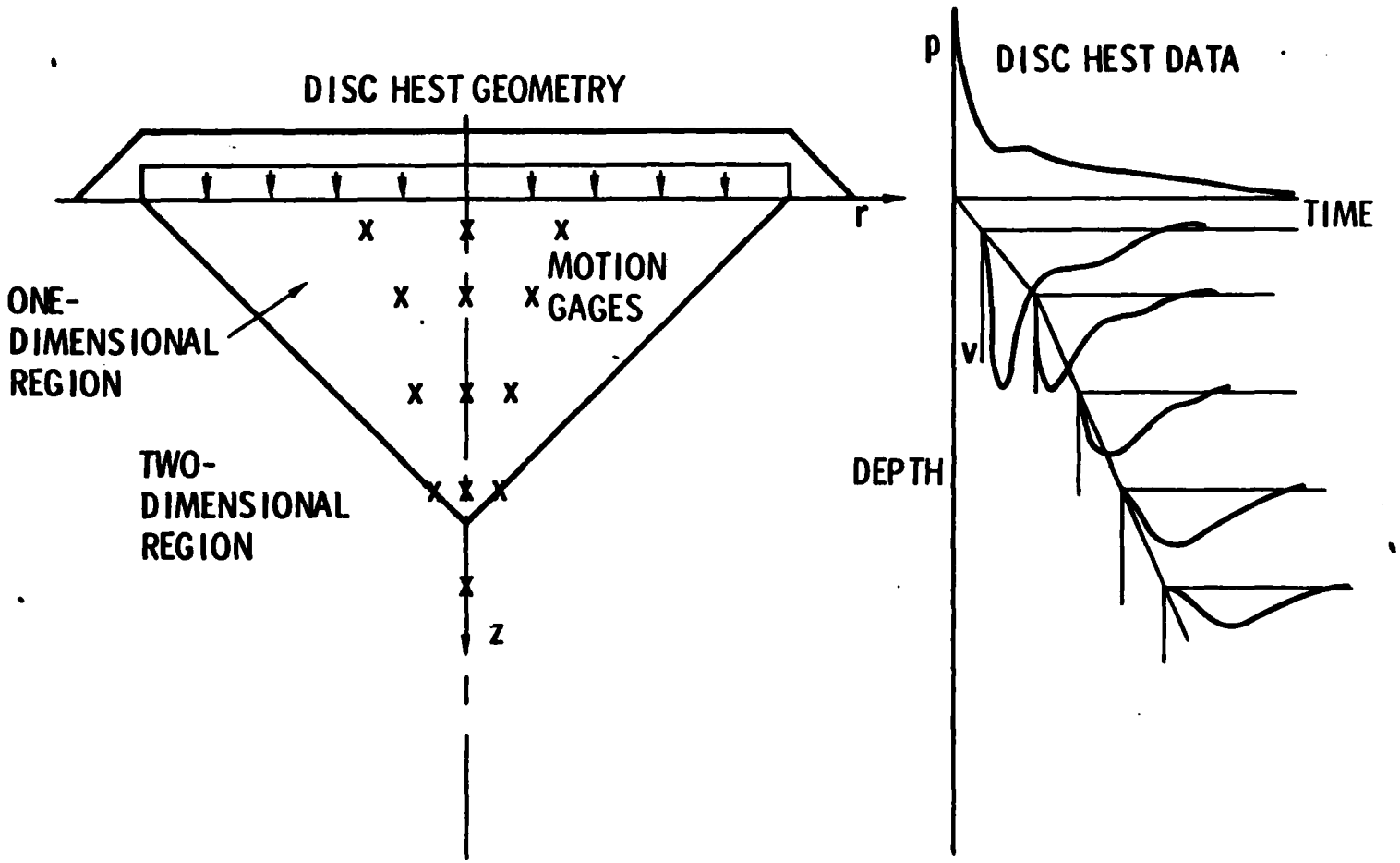

Fig. 1.-DISC HEST Test

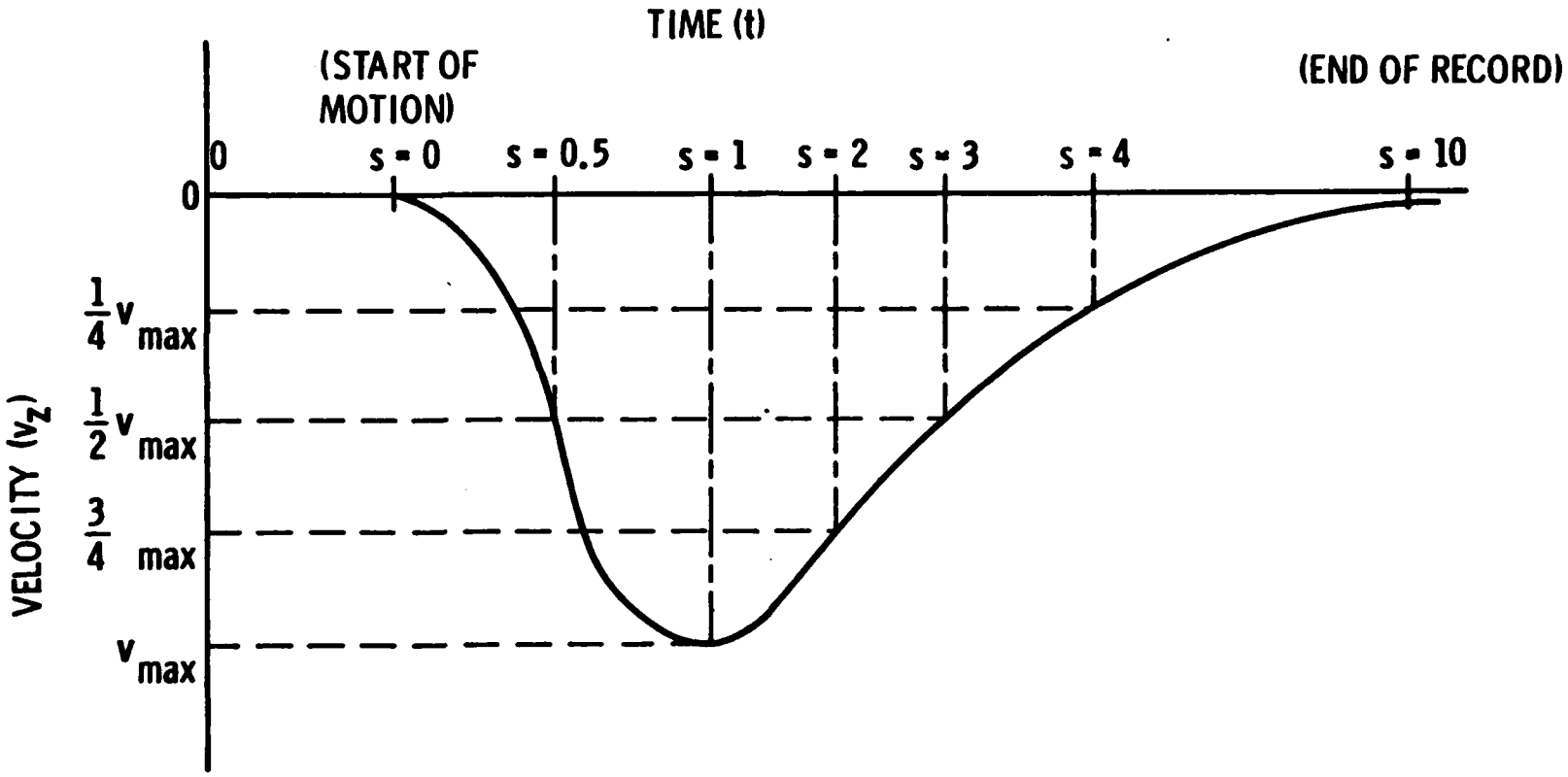

Fig. 2.-Typical Velocity versus Time Response

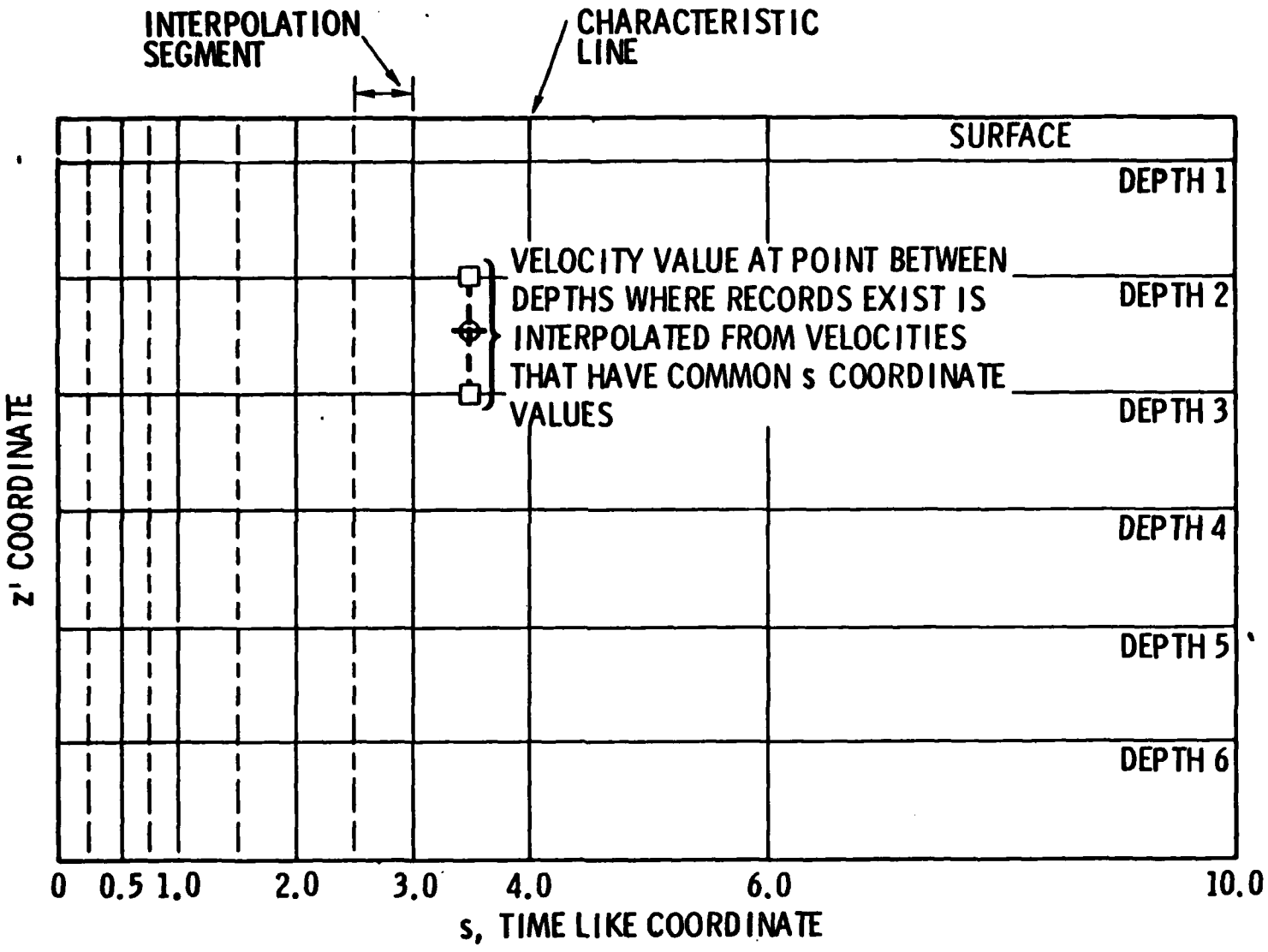

Fig. 3.-z', s Coordinate Space with Interpolation Segment Boundaries

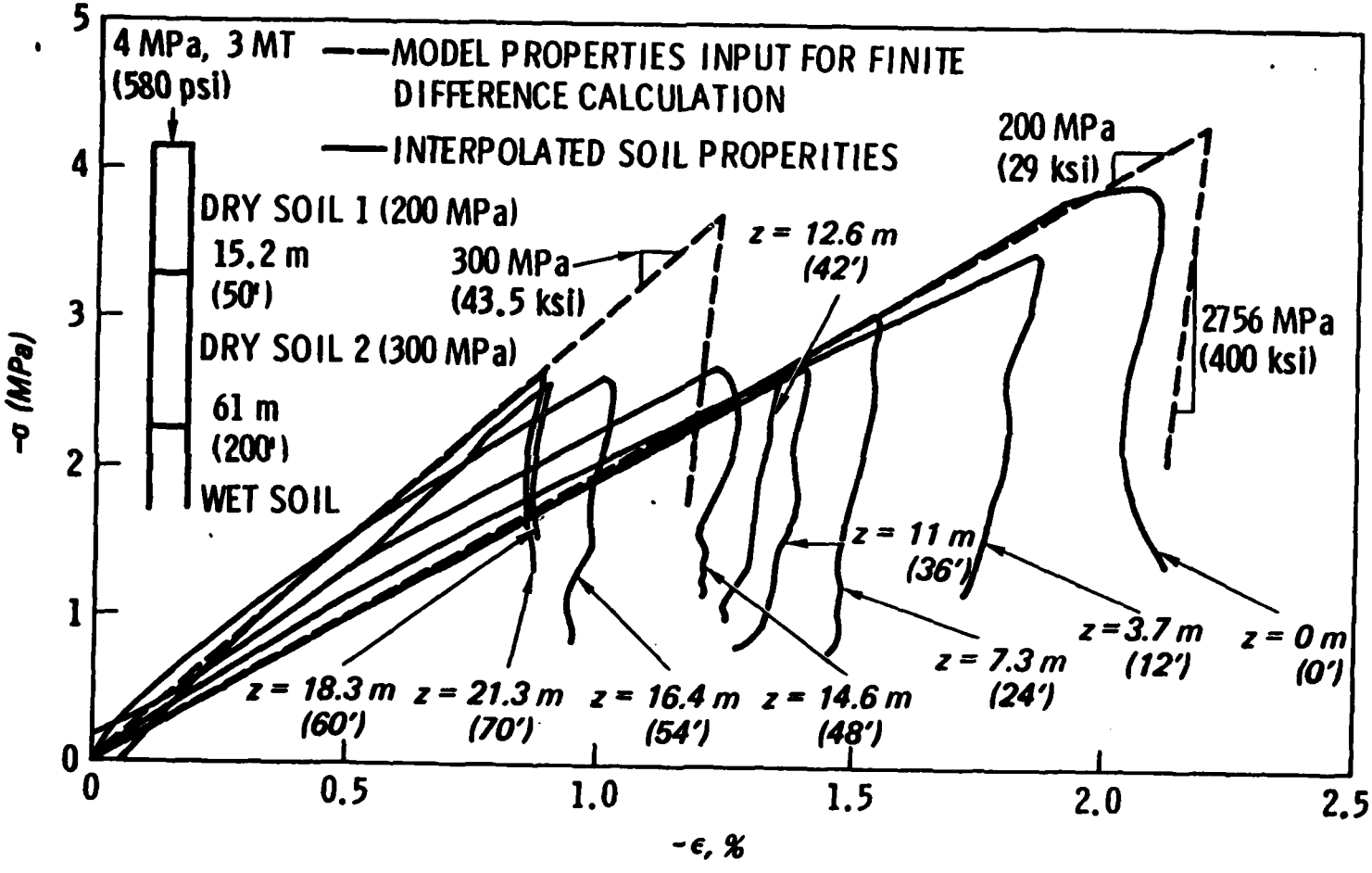

Fig. 4.-Comparison of Results for Layered Bilinear Material

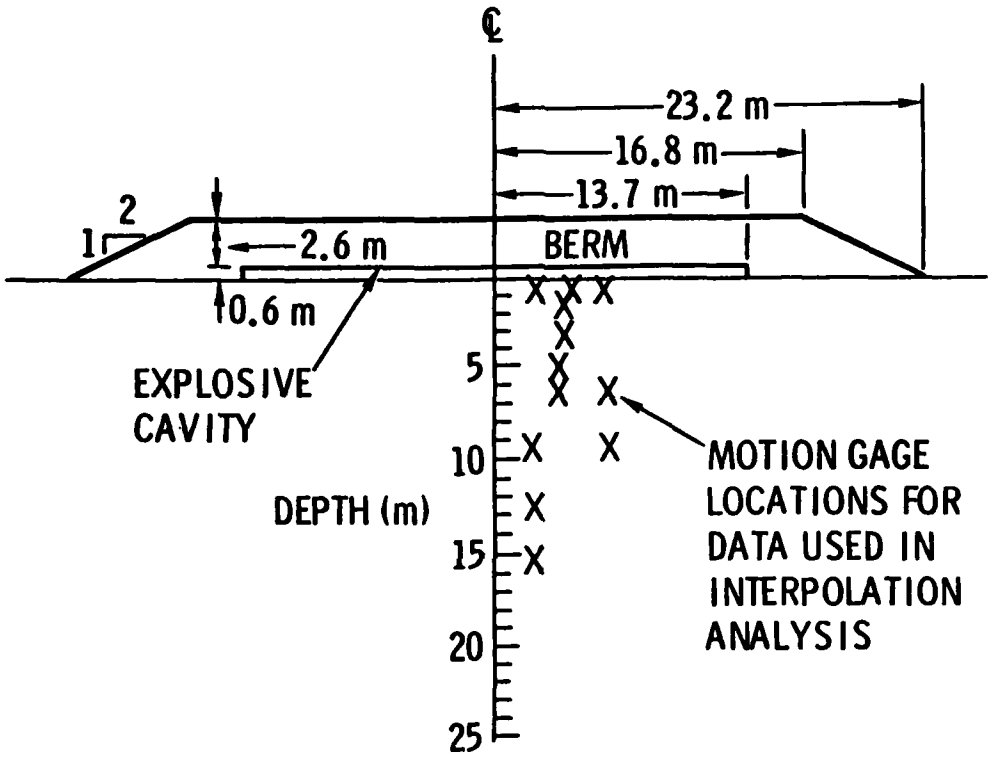

Fig. 5.-DISC HEST Test I

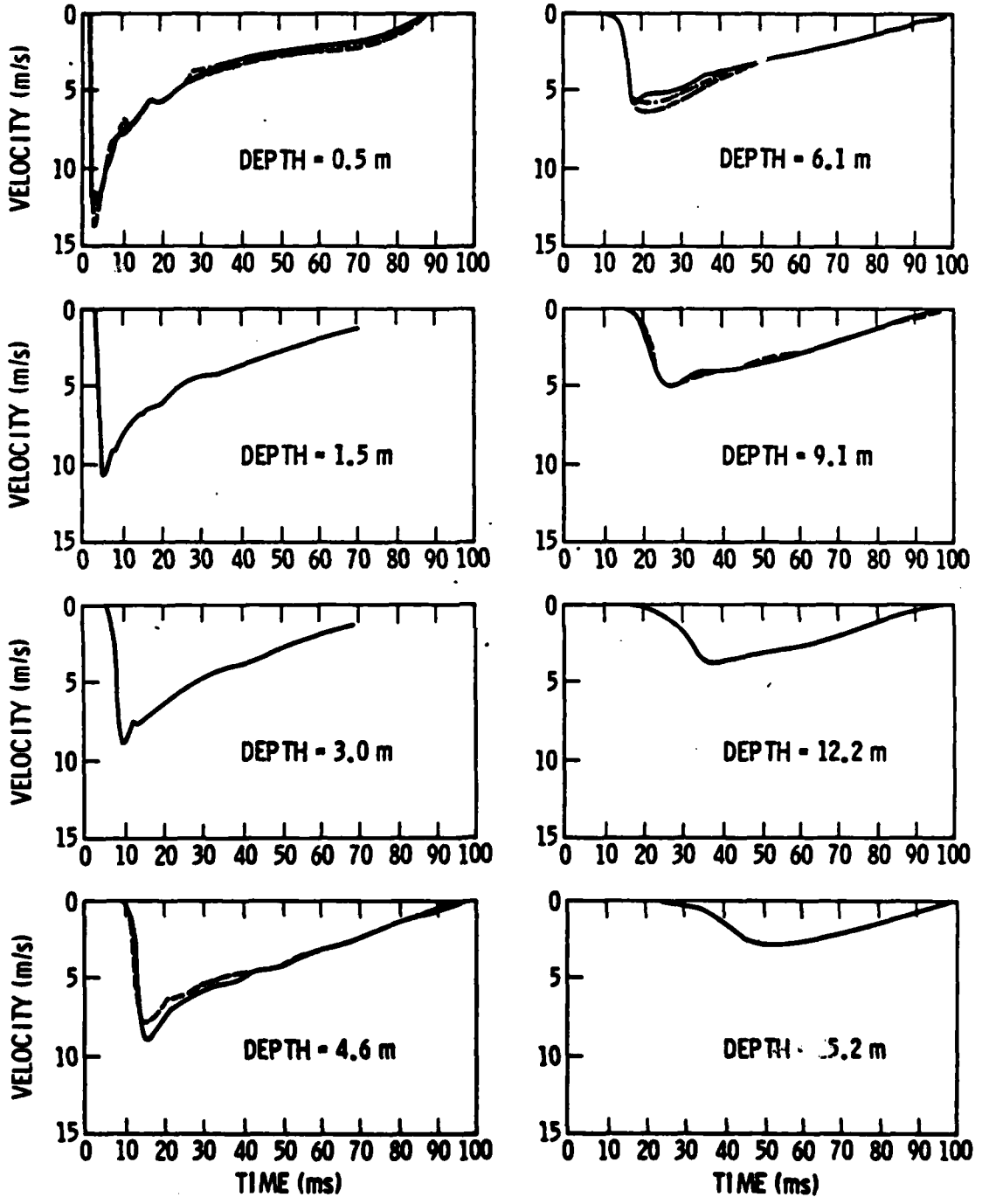

Fig. 6.-Velocity Records for DISC HEST Test I Analysis

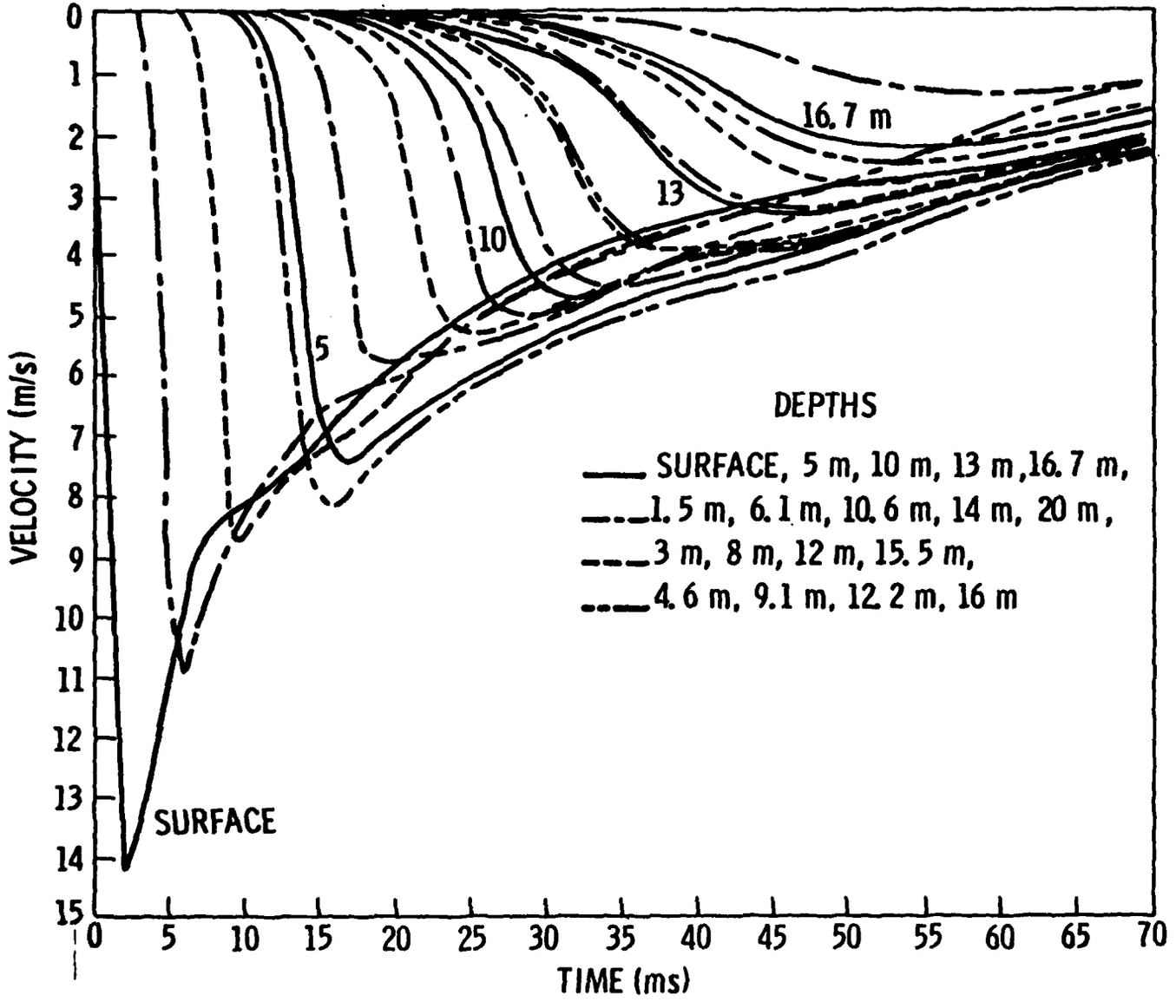

Fig. 7.-Interpolated Velocity History for DISC HEST Test I Analysis

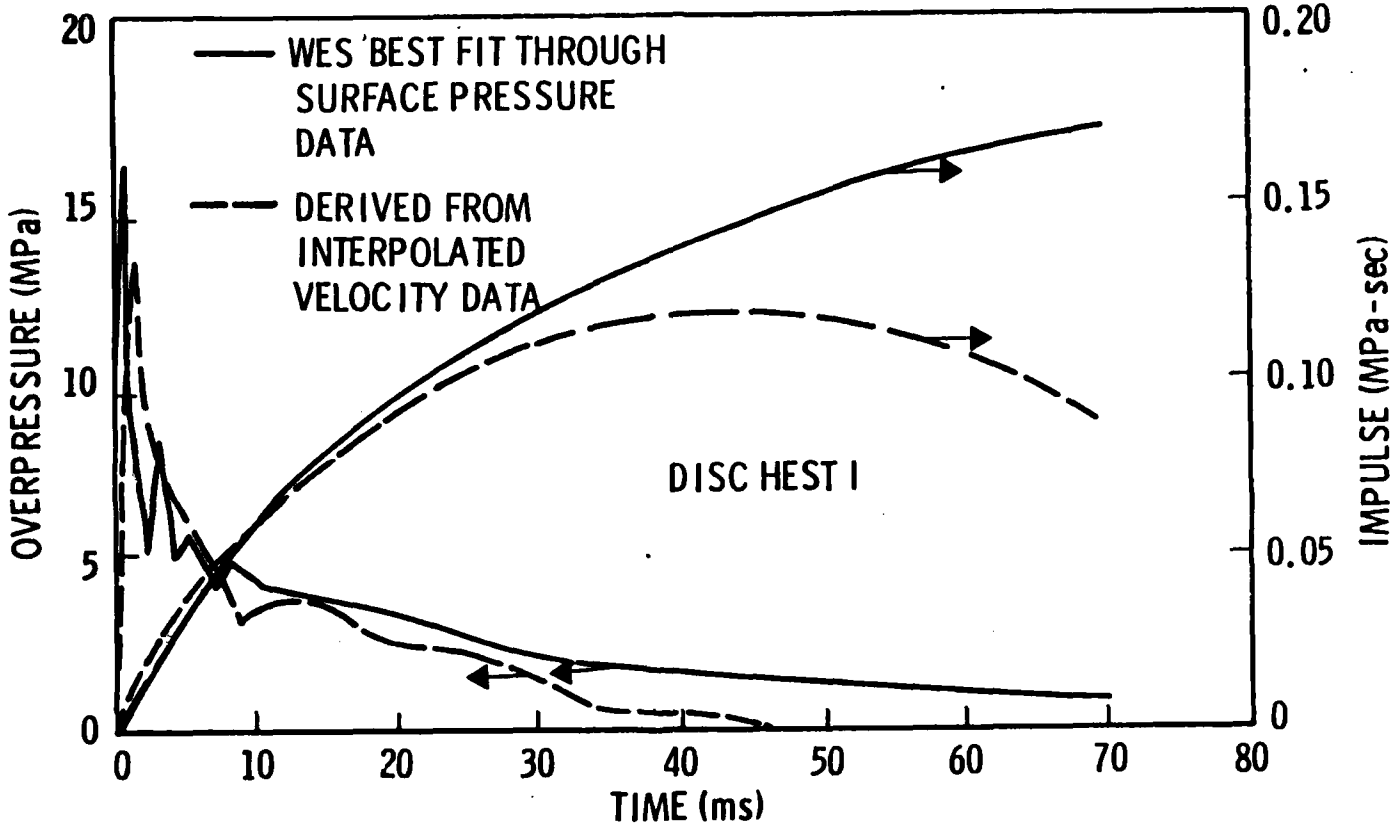

Fig. 8.-Surface Pressure and Impulse Comparison

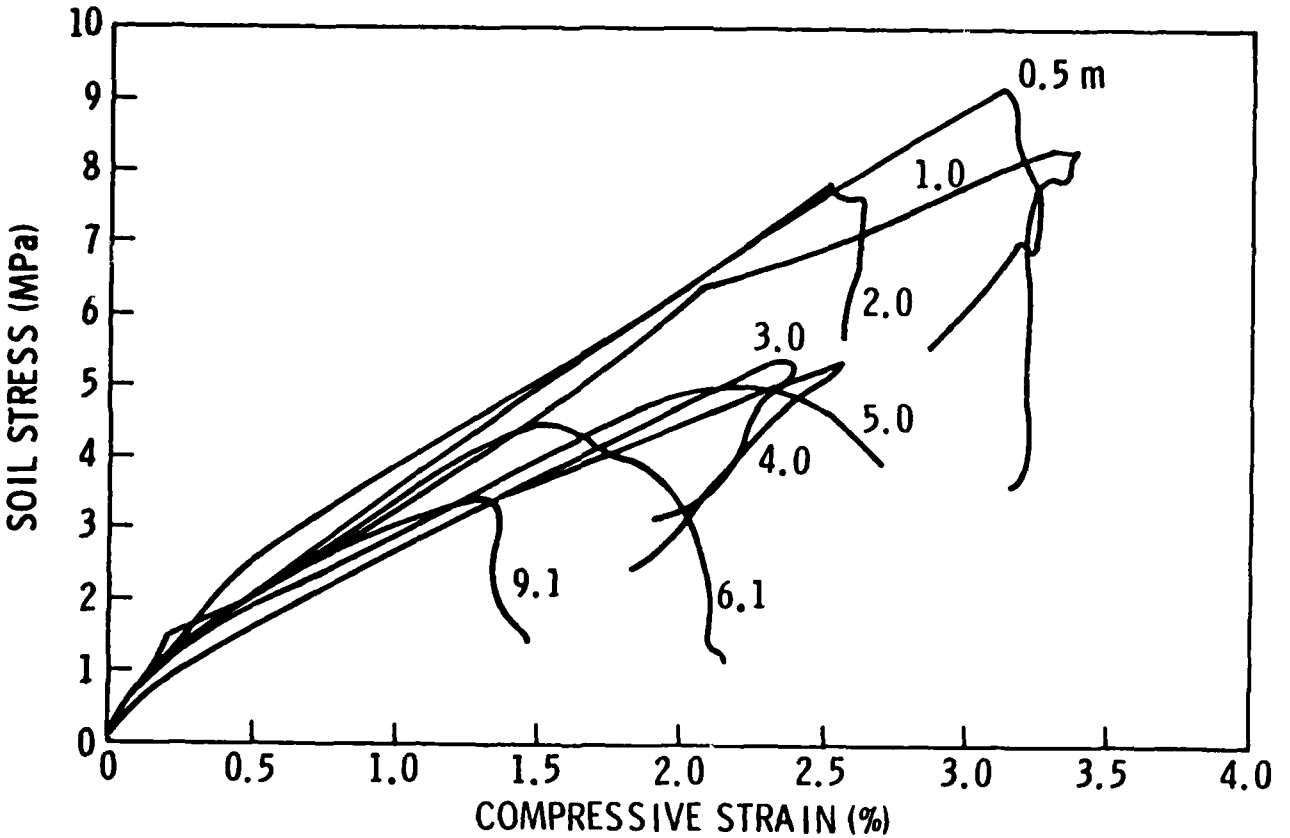

Fig. 9.-Soil Stress-Strain Histories for DISC HEST Test I

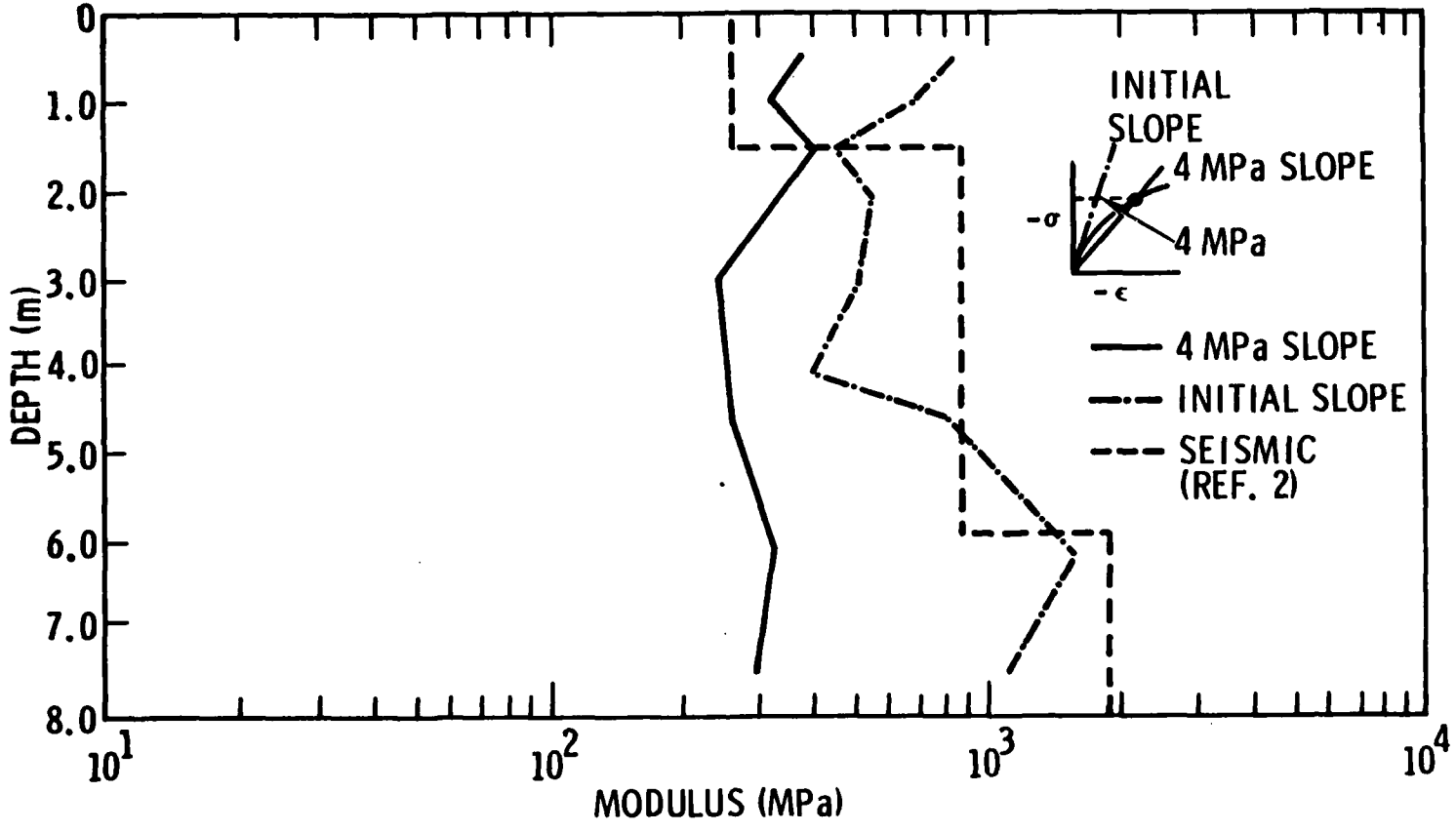

Fig. 10.-Soil Modulus versus Depth

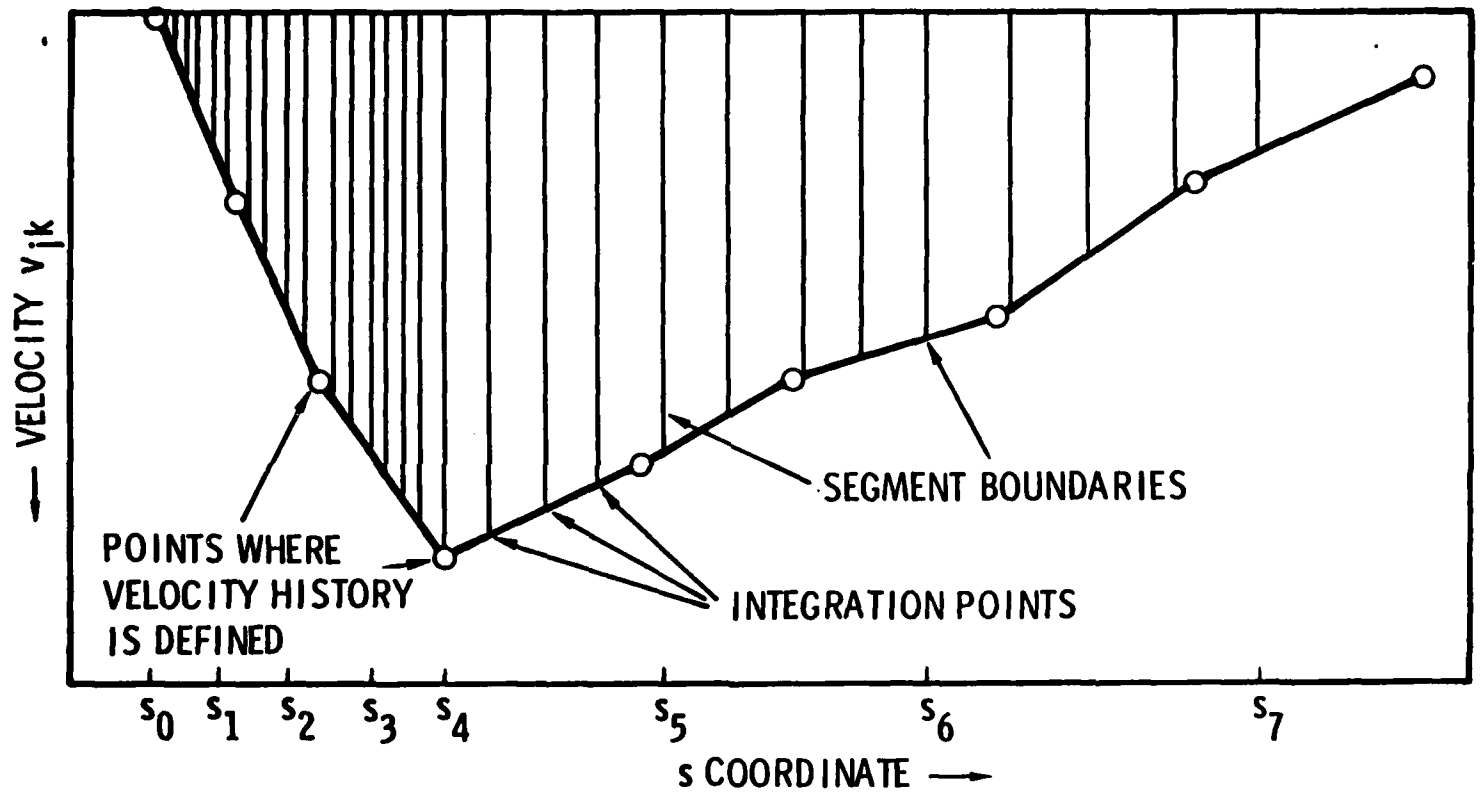

Fig. A-1.-Piecewise Definition of Velocity History

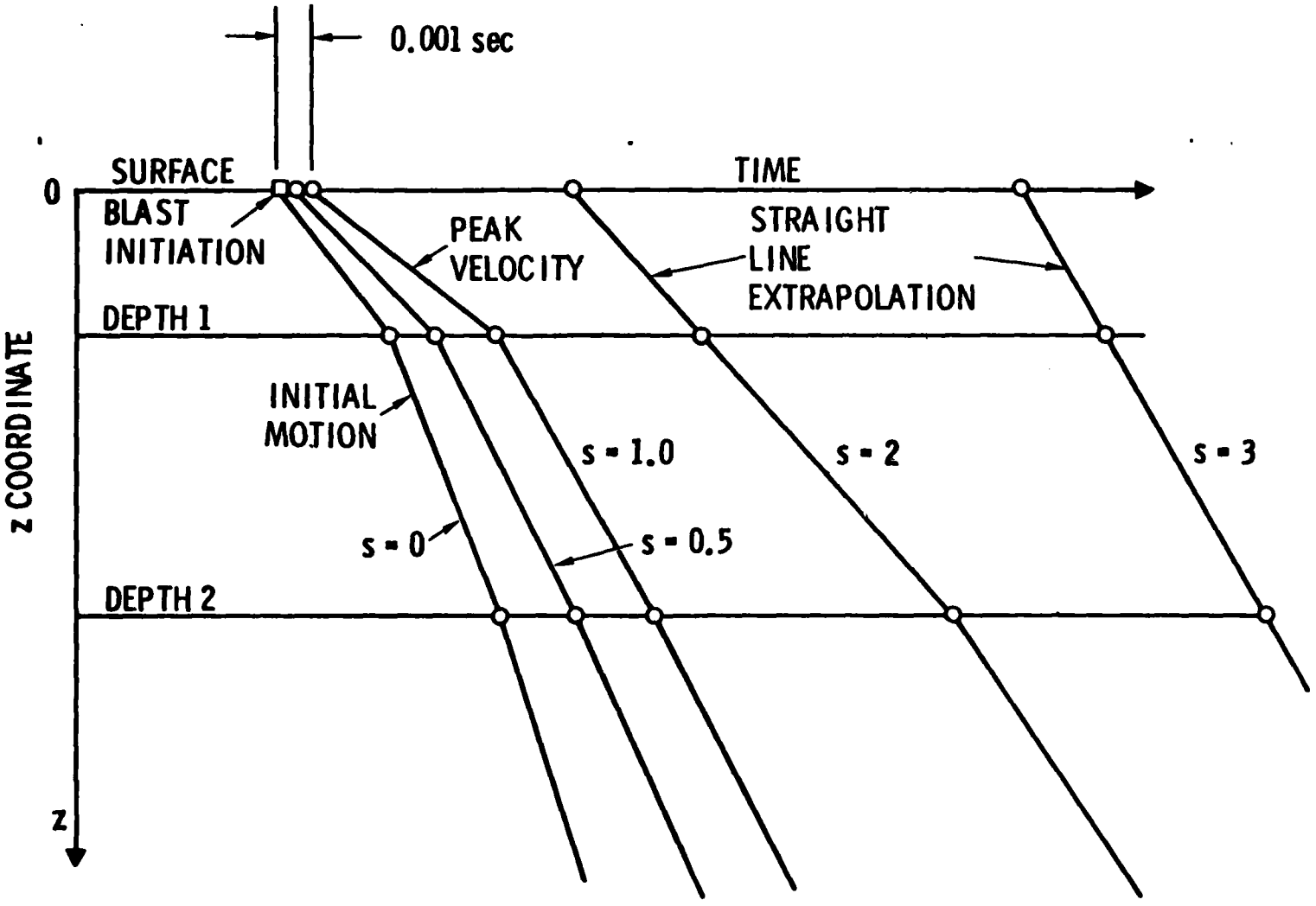

Fig. A-2.-s Label Configuration Between Surface and Shallowest Depths